

# Cellular automaton for chimera states

Vladimir García-Morales

Departament de Termodinàmica, Universitat de València,  
E-46100 Burjassot, Spain  
garmovla@uv.es

A minimalistic model for chimera states is presented. The model is a cellular automaton (CA) which depends on only one adjustable parameter, the range of the nonlocal coupling, and is built from elementary cellular automata and the majority (voting) rule. This suggests the universality of chimera-like behavior from a new point of view: Already simple CA rules based on the majority rule exhibit this behavior. After a short transient, we find chimera states for arbitrary initial conditions, the system spontaneously splitting into two stable phases separated by static boundaries, one synchronously oscillating and the other incoherent. When the coupling range is local, nontrivial coherent structures with different periodicities are formed.

Chimera states arise in sets of identical oscillators as a result of their stable grouping into two separated subsets, one of them synchronously oscillating, the other incoherent. This phenomenon was first pointed out in a network of oscillators under a symmetric nonlocal coupling [1, 2]. One decade after those seminal works, chimera states were first experimentally discovered in populations of coupled chemical oscillators [3] and in optical coupled-map lattices realized by liquid-crystal light modulators [4]. A vast amount of work on this subject, both theoretical [5–31] and experimental [32–40] has been produced since. Outside the laboratory, chimera states may describe some aspects of the dynamical behavior of social systems [41], power grids [42], epileptic seizures [43] and the unihemispheric sleep of birds and dolphins [44].

Chimera states have been mainly modeled in the past with differential equations and coupled map lattices. These models usually employ transcendental functions over real numbers. Because of their complexity, intensive numerical simulations and detailed bifurcation analyses are necessary to locate and characterize the chimeras in parameter space. The question then arises whether a simple and economic model exists that captures the main features of their dynamical behavior. In a previous work [22] we applied our phenomenological theory of complexity for cellular automata in an attempt to establish such a cellular automaton for chimera states. However, in our previous model [22] we found chimera states only for selected, specific initial conditions, and the domain walls bounding the spatial extension of the chimera were not stable (but presented nontrivial contractions and expansions). Furthermore, the relationship of that model to more elementary, Boolean cellular automata was not attempted and, finally, the connection of that model to the more general problem of phase separation was not considered.

In this article we tackle these problems through the formulation of a minimalistic model for chimera states, starting from building blocks which are elementary Boolean cellular automata (CAs) [45–53] with well known behavior. The model yields a universal mechanism for the spontaneous emergence of chimera states for any *arbitrary* initial condition. This is linked to the fact that we directly connect the emergence of chimera states to phase separation in spatially extended systems, a behavior that is statistically robust for generic initial conditions. The chimera states found here are *stable* and coexist with a uniformly oscillating synchronous phase from which it is separated by static and stable walls. The model is only dependent on one free parameter, the natural number  $\xi$  ( $\xi \geq 1$ ) whose physical meaning is the neighborhood radius (nonlocal coupling range). This parameter is related to the size of the domains formed. All structures here found are necessarily periodic because both local and global phase spaces are finite. When  $\xi$  is small, highly nontrivial coherent structures of small periodicity are formed. However when  $\xi$  is sufficiently large, domains with very large period compared to the base oscillation are formed.

We consider a ring with a number  $N_s$  of sites. The initial condition of a Boolean cellular automaton is contained in the vector  $\mathbf{x}_0 = (x_0^1, \dots, x_0^{N_s})$ , where each of the  $x_0^j \in \{0, 1\}$  denotes the initial dynamical state of the site  $j \in [0, N_s - 1]$  (the label  $j$  specifies the position of the site in the ring and it is always taken in this work modulo  $N_s$ ). At each discrete time  $t$ , the vector  $\mathbf{x}_t = (x_t^1, \dots, x_t^{N_s})$  specifies the state of the CA. A 1D cellular automaton  $f$  is a map which provides the local value  $x_{t+1}^j$  as a function of  $x_t^j$  and of the values on  $\xi$  sites to the left and to the right of  $x_t^j$ , i.e.

$$x_{t+1}^j = f \left( x_t^{j+\xi}, x_t^{j+\xi-1}, \dots, x_t^j, \dots, x_t^{j+1-\xi}, x_t^{j-\xi} \right) \quad (1)$$

Thus the natural number  $\xi$  specifies the radius of the neighborhood, which consists of  $2\xi + 1$  sites.

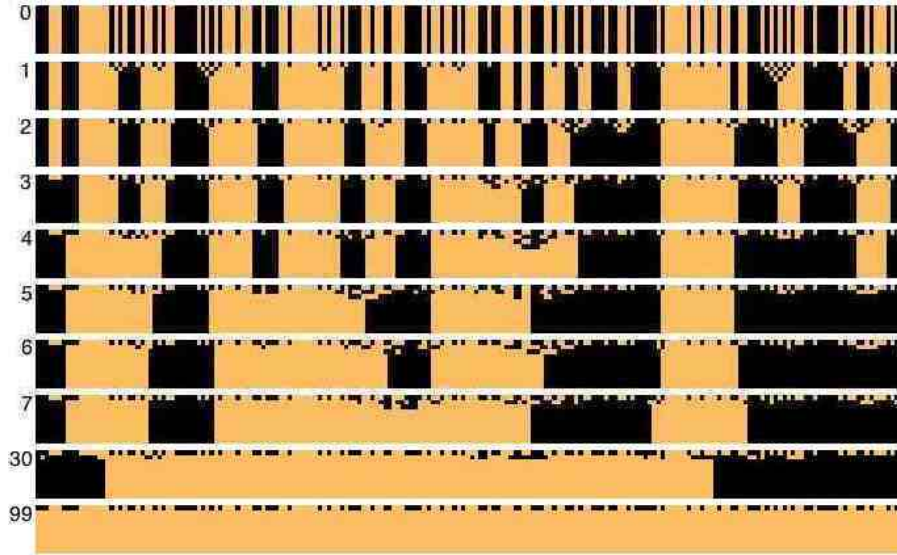


FIG. 1: Ten iterates of the majority rule, Eq. (2), for a ring of  $N_s = 200$  sites starting from a random initial condition (which is the same for all panels) for the values of  $\xi$  indicated in the figure. Sites with  $x_t^j = 1$  are light and those with  $x_t^j = 0$  are dark. Time flows from top to bottom in each panel.

Our approach combines three different Boolean CAs that we present first. The majority (voting) rule in 1D provides the phase separation mechanism and is given by

$$x_{t+1}^j = H \left( -\frac{1}{2} + \frac{1}{2\xi + 1} \sum_{k=-\xi}^{\xi} x_t^{j+k} \right) \quad (2)$$

where  $H(x)$  is the Heaviside function  $H(x) = 1$  for  $x < 1$ ,  $H(0) = \frac{1}{2}$  and  $H(x) = 0$  for  $x > 0$ . The spatiotemporal evolution of this rule for a random initial condition of zeros and ones is shown in Fig. 1 for the values of  $\xi$  indicated in the figure. It is well-known that the majority rule has a spatial fixed point consisting of domains of sites with value '1' and value '0' [47, 54, 55]. This is clearly observed in Fig. 1: After a short transient the system converges to a spatial fixed point where the size of the domains is on average, larger for  $\xi$  large. If  $\xi = \lfloor N_s/2 \rfloor$  with  $N_s$  odd (i.e. if  $N_s = 2\xi + 1$ ), the neighborhood of  $x_t^j$  coincides with the whole ring in which case we have a *global coupling*. Let  $N_1$  be the total number of sites with initial value '1' and  $N_0$  the sites with initial value '0' so that  $N_s = N_0 + N_1$ . Under global coupling, trivially, there is only a single domain, with all sites equal to one if the initial density  $\rho = N_1/N_s > 0.5$  or all sites equal to zero if  $\rho < 0.5$  (note that  $\rho = 0.5$  is not possible for  $N_s$  an odd number).

The following CA, that we shall also use in the model, generates oscillations that are uniform within a domain

$$x_{t+1}^j = 1 - H \left( -\frac{1}{2} + \frac{1}{2\xi + 1} \sum_{k=-\xi}^{\xi} x_t^{j+k} \right) \quad (3)$$

This CA is based on the majority rule above but generates oscillations between values '0' and '1', having no fixed-points. It is trivial to show that Eq. (3) has a 2-cycle once one has shown that the majority rule Eq. (2) has a fixed point. For, by noting that  $H(-x) = 1 - H(x)$ , and it-

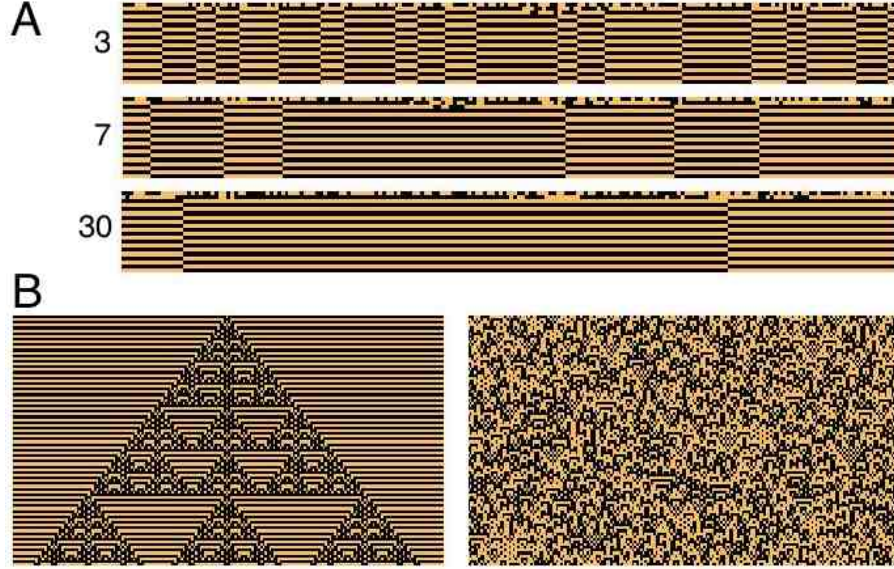


FIG. 2: A. Spatiotemporal evolution of the oscillating rule, Eq. (3), for values of  $\xi$  indicated in the figure and 20 time steps. The initial condition is the same as in Fig. (1). B. Spatiotemporal evolution of Wolfram's rule 105, Eq. (4) for a simple initial condition of a single site with value '1' surrounded by zeroes (left panel) and a generic initial condition (right panel) that is the same as in Fig. 1.

erating Eq. (3) twice, we find  $x_{t+2} = 1 - H\left(\frac{1}{2} - \frac{1}{2\xi+1} \sum_{k=-\xi}^{\xi} H\left(-\frac{1}{2} + \frac{1}{2\xi+1} \sum_{k'=-\xi}^{\xi} x_t^{j+k+k'}\right)\right) = H\left(-\frac{1}{2} + \frac{1}{2\xi+1} \sum_{k=-\xi}^{\xi} H\left(-\frac{1}{2} + \frac{1}{2\xi+1} \sum_{k'=-\xi}^{\xi} x_t^{j+k+k'}\right)\right)$  which is equal to two iterates of Eq. (2) as well. Thus, at the fixed point of Eq. (2) we have a 2-cycle of Eq. (3).

In Fig. 2 A the spatiotemporal evolution of this rule is shown for several different values of  $\xi$ . Domains are formed as in the majority rule case, (compare with Fig. 1) but each individual site instead of being at a fixed point, synchronously oscillates in phase with all sites within its same domain. Eq. (4) can be considered as a toy model for phase clusters in absence of phase balance, as it was described for the Belousov-Zhabotinsky reaction under global feedback [56].

Finally, the third CA that we shall use in the model is Wolfram rule 105, which is known to produce chaotic complex patterns (Class 3 behavior) [45, 57]

$$x_{t+1}^j = \mathbf{d}_2\left(0, 1 + x_t^{j+1} + x_t^j + x_t^{j-1}\right) \quad (4)$$

where

$$\mathbf{d}_p(k, x) = \left\lfloor \frac{x}{p^k} \right\rfloor - p \left\lfloor \frac{x}{p^{k+1}} \right\rfloor \quad (5)$$

is the digit function [58–60], the brackets  $\lfloor \dots \rfloor$  denoting the floor (lower closest integer) function, and where  $p > 1$  is a natural number,  $k$  an integer and  $x$  a real number. Since  $x = 1 + x_t^{j+1} + x_t^j + x_t^{j-1}$  in Eq. (4) is an integer, the digit function is similar in this case to the mod 2 operation, and one can equivalently write that equation as  $x_{t+1}^j = 1 + x_t^{j+1} + x_t^j + x_t^{j-1} \pmod{2}$ . In terms of the digit function, any CA rule with Wolfram code  $R \in [0, 255]$  can be succinctly written as  $x_{t+1}^j = \mathbf{d}_2(4x_t^{j+1} + 2x_t^j + x_t^{j-1}, R)$  (see [60]). Rule 105 is selected because, being chaotic and of Class 3, it sends the neighborhood configurations '000' to '1' and '111' to '0' and, thus, it also possess a homogeneous 2-cycle as solution,

as Eq. (3) does. The spatiotemporal evolution of Eq. (4) is shown in Fig. 2 B for a simple initial condition consisting of a single site with value '1' surrounded by zeroes (left panel) and an arbitrary initial condition (right panel) that is the same as in Fig. 1. Although a nested regular pattern is observed in the former case, strongly incoherent behavior is found in the latter one. This is typical of a Wolfram Class 3 rule, which, due to their spatiotemporal incoherence, behave well as (pseudo)random number generators [45, 57]. We also note in the left panel, the presence of the 2-cycle, coexisting with the nested structure.

We now explain how the three CA described above, Eqs. (2) to (4) can be combined together to construct a meaningful model for chimera states. We summarize the main results contained in [60] of relevance here and refer the interested reader to [60] for more details. In [60] we have noted that if  $x$  is an integer between 0 and  $p - 1$ , and  $p = p_0 p_1 p_2$ , then we can find  $a^{(0)} \in [0, p_0 - 1]$ ,  $a^{(1)} \in [0, p_1 - 1]$  and  $a^{(2)} \in [0, p_2 - 1]$  integers such that

$$x = a^{(0)} + p_0 a^{(1)} + p_0 p_1 a^{(2)} \quad (6)$$

and so that the numbers  $a^{(0)}$ ,  $a^{(1)}$ ,  $a^{(2)}$  can be obtained *from the knowledge of  $x$  only* as

$$\begin{aligned} a^{(0)} &= \mathbf{d}_{p_0}(0, x) \\ a^{(1)} &= \mathbf{d}_{p_1}\left(0, \frac{x}{p_0}\right) \\ a^{(2)} &= \mathbf{d}_{p_2}\left(0, \frac{x}{p_0 p_1}\right) \end{aligned}$$

Now, let  $x_t^j \in [0, 7]$  be the output at each location  $j$  and time  $t$  of a CA working on  $p = 8$  symbols. It is then clear that we can write  $x_t^j = a_t^{(0),j} + 2a_t^{(1),j} + 4a_t^{(2),j}$  at every time and location, so that  $a_t^{(0),j}$ ,  $a_t^{(1),j}$  and  $a_t^{(2),j}$  are all Boolean variables. In [60] such quantities are called *layers*. We also use the important fact that Boolean variables are idempotent under ordinary multiplication and that the product of two Boolean quantities is also a Boolean quantity.

Let then  $\varphi_t^j = 2\pi x_t^j / 8$  denote the discrete phase of an oscillator in the unit circle, with  $x_t^j \in [0, 8]$  an integer. We thus consider the unit circle as discretized into eight equal sectors. We model chimera states by means of the following CA

$$x_{t+1}^j = y_{t+1}^{(0),j} + 2 \left(1 - y_{t+1}^{(0),j}\right) y_{t+1}^{(1),j} + 4 y_{t+1}^{(0),j} y_{t+1}^{(2),j} \quad (7)$$

where the  $y_{t+1}^{(h),j}$  are Boolean variables ( $j \in [0, N_s - 1]$ ) given by the maps

$$y_{t+1}^{(0),j} = H \left( -\frac{1}{2} + \frac{1}{2\xi + 1} \sum_{k=-\xi}^{\xi} y_t^{(0),j+k} \right) \quad (8)$$

$$y_{t+1}^{(1),j} = 1 - H \left( -\frac{1}{2} + \frac{1}{2\xi + 1} \sum_{k=-\xi}^{\xi} y_t^{(1),j+k} \right) \quad (9)$$

$$y_{t+1}^{(2),j} = \mathbf{d}_2 \left( 0, 1 + y_t^{(2),j+1} + y_t^{(2),j} + y_t^{(2),j-1} \right) \quad (10)$$

and where,

$$y_t^{(0),j} = \mathbf{d}_2(0, x_t^j) \quad (11)$$

$$y_t^{(1),j} = \mathbf{d}_2\left(0, \frac{x_t^j}{2}\right) \quad (12)$$

$$y_t^{(2),j} = \mathbf{d}_2\left(0, \frac{x_t^j}{4}\right) \quad (13)$$

so that, initially,  $y_0^{(0),j} = \mathbf{d}_2(0, x_0^j)$ ,  $y_0^{(1),j} = \mathbf{d}_2\left(0, \frac{x_0^j}{2}\right)$ ,  $y_0^{(2),j} = \mathbf{d}_2\left(0, \frac{x_0^j}{4}\right)$ . From the above scheme, the only necessary input is, thus, the initial condition  $x_0^j$  and the parameter  $\xi$ . The output of the CA is  $x_t^j$  at every  $t$  and  $j$ . If we compare Eqs. (6) and (7), we have  $a_t^{(0),j} = y_t^{0,j}$ ,  $a_t^{(1),j} = \left(1 - y_t^{(0),j}\right) y_t^{(1),j}$  and  $a_t^{(2),j} = y_t^{(0),j} y_t^{(2),j}$  for  $t \geq 1$  and  $a_0^{(0),j} = y_0^{0,j}$ ,  $a_0^{(1),j} = y_0^{(1),j}$ ,  $a_0^{(2),j} = y_0^{(2),j}$  at  $t = 0$ . Furthermore, we see that Eqs. (8), (9) and (10) correspond to Eqs. (2), (3) and (4), respectively. Indeed the layers of the CA can be directly extracted at any time  $t > 0$  from  $x_t^j$  since, from Eq. (7)

$$y_{t+1}^{(0),j} = \mathbf{d}_2(0, x_{t+1}^j) \quad (14)$$

$$\left(1 - y_{t+1}^{(0),j}\right) y_{t+1}^{(1),j} = \mathbf{d}_2\left(0, \frac{x_{t+1}^j}{2}\right) \quad (15)$$

$$y_{t+1}^{(0),j} y_{t+1}^{(2),j} = \mathbf{d}_2\left(0, \frac{x_{t+1}^j}{4}\right) \quad (16)$$

In Fig. 3 the spatiotemporal evolution of Eq. (7) is shown for different values of the coupling range,  $\xi = 30$  (A), 7 (B) and 1 (C), for  $N_s = 200$  sites and 400 time steps and for a generic initial condition (see figure caption). We observe in the figure that, although the model dynamics over all sites is identical (note that, besides the global translation invariance  $j \rightarrow j + N_s$  the model is invariant under any finite shift  $j \rightarrow j + h$ , for any  $h$  integer) after few time steps the system spontaneously splits into two different phases, one uniformly oscillating and the other incoherent. The walls separating the domains are stable, as are the chimera states thus formed. The size of the domains is related to the value of the coupling range: For larger coupling range, the domains are broader. Quite strikingly, when  $\xi$  is small, e.g.  $\xi = 1$  as in panel C, complex coherent structures with well defined periodicity are observed. In the leftmost panel of Fig. 3 a detail of panel C is shown, where bands with thickness of 9, 7 and 10 sites contain structures with periods  $T = 12, 14$  and  $62$ , respectively, all these coherent structures coexisting with the uniformly oscillating background of period 2. We can explain this behavior due to the deterministic, error-free computation over a finite phase space. Let an inhomogeneous band be a number  $n$  of sites thick. Then, because of the finiteness of the dynamics, the period is bounded as  $T \leq 2^n$ , where the equality would only hold if the dynamics were ergodic (which is not). For the chimera state in panel A of Fig. 3 we would expect the pattern to be repeated before  $\sim 2^{140}$  time steps (we have continued the simulation finding no periodicity for any reasonable computation time).

A dynamical ‘dissection’ of the model is shown in Fig. 4. Panel A of that figure is a detail of panel C of Fig. 3 for the first 20 iteration steps. The spatiotemporal evolution of the layers, as obtained from Eqs. (14) to (16) are shown by plotting, respectively,  $\mathbf{d}_2(0, x_t^j)$  (panel B),  $\mathbf{d}_2(0, x_t^j/2)$  (panel C) and  $\mathbf{d}_2(0, x_t^j/4)$  (panel D). We see that  $x_t^j$  depends on the output of the majority rule (panel B)

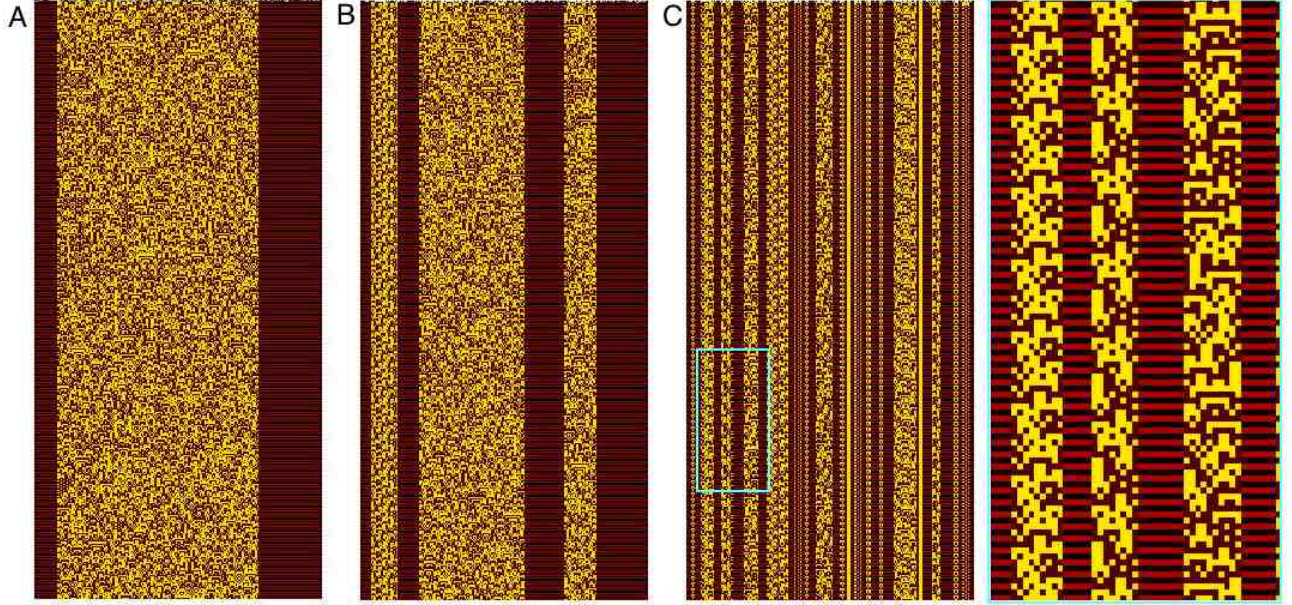


FIG. 3: Spatiotemporal evolution of  $x_t^j$  provided by Eq. (7) for  $\xi = 30$  (A), 7 (B) and 1 (C), for  $N_s = 200$  sites and 400 time steps and for an initial condition  $x_0^j = a^j + 2a^j + 4a^j$ , where  $a^j \in \{0, 1\}$  is as in Fig. (1). The rightmost panel is a detail of panel C, showing some complex coherent periodic structures with periods  $T = 12, 14$  and  $62$ .



FIG. 4: Detail of the spatiotemporal evolution of the CA dynamics for the first 20 time steps of panel C in Fig. 3: Spatiotemporal evolution  $x_t^j$  (A),  $\mathbf{d}_2(0, x_t^j)$  (B),  $\mathbf{d}_2(0, x_t^j/2)$  (C) and  $\mathbf{d}_2(0, x_t^j/4)$  (D).

as follows: *If the output  $y_t^{(0),j}$  of the majority rule dictated by Eq. (8) is '0',  $x_t^j$  takes a uniformly oscillating value governed by Eq. (9); if the output  $y_t^{(0),j}$  is '1',  $x_t^j$  is found in the incoherent phase and takes a value governed by Eq. (10).*

After our result in [60], Eq. (7) exactly corresponds to a CA on a finite alphabet over eight values and with nonlocal range  $2\xi + 1$ . We remark that although the model is directly understood from its design, its local dynamical behavior is highly nontrivial because of the interaction of the

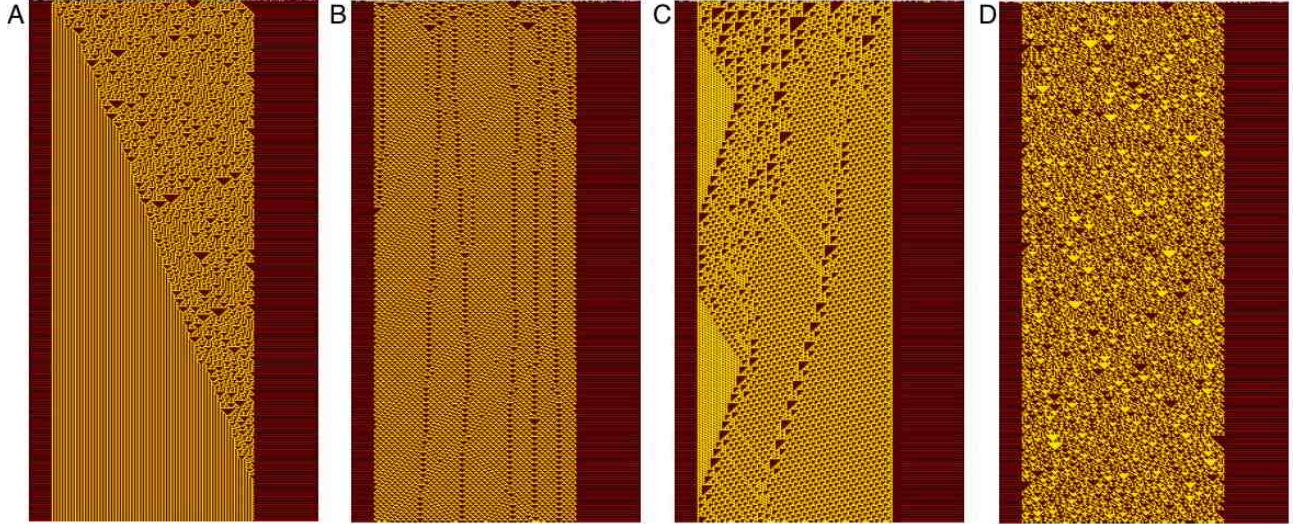


FIG. 5: Spatiotemporal evolution of  $x_t^j$ , as obtained from Eqs. (7), (8), (9) and (17) for  $\xi = 30$  and  $R = 30$  (A),  $R = 110$  (B),  $R = 54$  (C) and  $R = 150$  (D) for the same random initial condition, number of time steps and system size as in Fig. 3

domain borders with the structures formed inside the incoherent region. Specially, the appropriate Class 3 rule, Wolfram's 105 rule, had to be chosen to warrant that incoherence does not disappear through interaction with the borders. Such Class 3 rule is chaotic, but has certain regularities, as revealed by the addition modulo 2 operation in Fig. 2B (left). There are many other possible choices for maps depending on the addition modulo 2 operation that would lead to a similar qualitative behavior. We have chosen a Class 3 CA rule that a) has the uniform oscillation as possible solution and b) is localized. Now we consider the fate of other more complex CA rules, some believed to be computationally irreducible. To investigate them we replace Eq. (10) in the model by

$$y_{t+1}^{(2),j} = \mathbf{d}_2(4y_t^{(2),j+1} + 2y_t^{(2),j} + y_t^{(2),j-1}, R) \quad (17)$$

so that we can study the model as a function of the Wolfram code  $R$ . In particular the rules with  $R = 30, 54$  and  $110$  are interesting because are supposed to be computationally irreducible. Rule 30 is an efficient random number generator, rule 110 is known to be a universal Turing machine and Rule 54 is a Class 4 rule which is conjectured to be able to perform universal computation as well [45]. In Fig. 5 the spatiotemporal evolution of  $x_t^j$  is plotted as obtained from Eqs. (7), (8), (9) and (17) for  $\xi = 30$  and  $R = 30$  (panel A),  $R = 54$  (panel B),  $R = 110$  (panel C) and  $R = 150$  (panel D) for the same random initial condition as in Fig. 3. We see that for rule 30 (panel A) the chaotic behavior within the incoherent phase dies out after less than 400 iterations through interaction with the borders. We note that rule 30 is asymmetric (i.e. it is not invariant under a left-right transformation) and therefore, this extinction process is also asymmetric and takes place on a privileged direction from left to right. Rules 54 and 110 are Class 4 rules with most complex behavior and consists on soliton-like complex coherent structures propagating on a regular background in generically unpredictable ways. Rule 54 is left-right symmetric and the collisions of the complex structures with the borders possess the same features. However, rule 100 is asymmetric and complex structures tend to stick and be remitted from the left border, collapsing on the right border of the domain. Finally, rule 150 (addition modulo 2 over the neighborhood sites) is fully incoherent and leads to a chimera state as well (although it does



not contain the homogeneous oscillation as 2-cycle).

In this article we have presented a minimalistic CA model for chimera states. For small values of the coupling range  $\xi$  (the only parameter in the model), we have found highly nontrivial coherent structures with observable periodicity. For intermediate values of  $\xi$ , however, the domains are broader and the inhomogeneous part is incoherent for any reasonable computation time and it is in this domain that chimera states are found. When the coupling range is equal to the system size (global coupling) no chimera states of the kind described here are possible because one has a single phase, either fully incoherent or uniformly oscillating. Recently, chimera states under global coupling have been experimentally found in electrochemical systems [37] and modeled employing a modified complex Ginzburg-Landau equation [61, 62] and Stuart-Landau oscillators [37]. However, in these models, the mechanism leading to the emergence of chimera states is different, since it is caused by the presence of a global constraint (the conservation of the homogeneous oscillation) which introduces nontrivial correlations, being the key element for the ensemble of oscillators to split into two (balanced) phases.

- 
- [1] Y. Kuramoto and D. Battogtokh, *Nonlin. Phen. in Complex Sys.* **5**, 380 (2002).
  - [2] D. M. Abrams and S. H. Strogatz, *Phys. Rev. Lett.* **93**, 174102 (2004).
  - [3] M. R. Tinsley, S. Nkomo, and K. Showalter, *Nature Phys.* **8**, 662 (2012).
  - [4] A. M. Hagerstrom *et al.*, *Nature Phys.* **8**, 658 (2012).
  - [5] D. M. Abrams and M. J. Panaggio, *Nonlinearity* **28**, R67 (2015).
  - [6] D. M. Abrams, R. E. Mirollo, S. H. Strogatz, and D. A. Wiley, *Phys. Rev. Lett.* **101**, 084103 (2008).
  - [7] G. C. Sethia, A. Sen, and F. M. Atay, *Phys. Rev. Lett.* **100**, 144102 (2008).
  - [8] C. R. Laing, *Physica D* **238**, 1569 (2009).
  - [9] A. E. Motter, *Nature Phys.* **6**, 164 (2010).
  - [10] E. A. Martens, C. R. Laing, and S. H. Strogatz, *Phys. Rev. Lett.* **104**, 044101 (2010).
  - [11] S. Olmi, A. Politi, and A. Torcini, *Europhys. Lett.* **92**, 60007 (2010).
  - [12] G. Bordyugov, A. Pikovsky, and M. Rosenblum, *Phys. Rev. E* **82**, 035205 (2010).
  - [13] J. H. Sheeba, V. K. Chandrasekar, and M. Lakshmanan, *Phys. Rev. E* **81**, 046203 (2010).
  - [14] M. Wolfrum and O. E. Omelchenko, *Phys. Rev. E* **84**, 015201 (2011).
  - [15] C. R. Laing, *Physica D* **240**, 1960 (2011).
  - [16] I. Omelchenko, Y. Maistrenko, P. Hövel, and E. Schöll, *Phys. Rev. Lett.* **106**, 234102 (2011).
  - [17] I. Omelchenko, B. Riemenschneider, P. Hövel, Y. Maistrenko, and E. Schöll, *Phys. Rev. E* **85**, 026212 (2012).
  - [18] I. Omelchenko, O. E. Omelchenko, P. Hövel, and E. Schöll, *Phys. Rev. Lett.* **110**, 224101 (2013).
  - [19] S. Nkomo, M. R. Tinsley, and K. Showalter, *Phys. Rev. Lett.* **110**, 224102 (2013).
  - [20] J. Hizanidis, A. Kanas, A. Bezerianos, and T. Bountis, *Int. J. Bifurcation Chaos* **24**, 1450030 (2014).
  - [21] G. C. Sethia, A. Sen, and G. L. Johnston, *Phys. Rev. E* **88**, 042917 (2013).
  - [22] V. García-Morales, *Phys. Rev. E* **88**, 042814 (2013).
  - [23] G. C. Sethia and A. Sen, *Phys. Rev. Lett.* **112**, 144101 (2014).
  - [24] A. Yeldesbay, A. Pikovsky, and M. Rosenblum, *Phys. Rev. Lett.* **112**, 144103 (2014).

- [25] F. Böhm, A. Zakharova, E. Schöll, and K. Lüdge, Phys. Rev. E **91**, 040901R (2015).
- [26] A. Buscarino, M. Frasca, L. V. Gambuzza, and P. Hövel, Phys. Rev. E **91**, 022817 (2015).
- [27] I. Omelchenko, A. Provata, J. Hizanidis, E. Schöll, and P. Hövel, Phys. Rev. E **91**, 022917 (2015).
- [28] I. Omelchenko, A. Zakharova, P. Hövel, J. Siebert, and E. Schöll, Chaos **25**, 083104 (2015).
- [29] P. S. Dutta and T. Banerjee, Phys. Rev. E **92**, 042919 (2015).
- [30] P. Ashwin and O. Burylko, Chaos **25**, 013106 (2015).
- [31] J. Hizanidis *et al.*, Phys. Rev. E **92**, 012915 (2015).
- [32] E. A. Martens, S. Thutupalli, A. Fourriere, and O. Hallatschek, Proc. Natl. Acad. Sci. USA **110**, 10563 (2013).
- [33] L. Larger, B. Penkovsky, and Y. Maistrenko, Phys. Rev. Lett. **111**, 054103 (2013).
- [34] T. Kapitaniak, P. Kuzma, J. Wojewoda, K. Czolczynski, and Y. Maistrenko, Sci. Rep. **4**, 6379 (2014).
- [35] M. Wickramasinghe and I. Z. Kiss, PLoS ONE **8**, e80586 (2013).
- [36] M. Wickramasinghe and I. Z. Kiss, Phys. Chem. Chem. Phys. **16**, 18360 (2014).
- [37] L. Schmidt, K. Schönleber, K. Krischer, and V. Garcia-Morales, Chaos **24**, 013102 (2014).
- [38] L. V. Gambuzza *et al.*, Phys. Rev. E **90**, 032905 (2014).
- [39] D. P. Rosin, D. Rontani, N. D. Haynes, E. Schöll, and D. J. Gauthier, Phys. Rev. E **90**, 030902R (2014).
- [40] L. Larger, B. Penkovsky, and Y. Maistrenko, Nature Commun. **6**, 7752 (2015).
- [41] J. C. Gonzalez-Avella, M. Cosenza, and M. S. Miguel, Physica A **399**, 24 (2014).
- [42] A. E. Motter, S. A. Myers, M. Anghel, and T. Nishikawa, Nature Phys. **9**, 191 (2013).
- [43] A. Rothkegel and K. Lehnertz, New J. Phys. **16**, 055006 (2014).
- [44] N. Rattenborg, C. J. Amlaner, and S. L. Lima, Neurosci. Biobehav. Rev. **24**, 817 (2000).
- [45] S. Wolfram, *A New Kind of Science* (Wolfram Media Inc., Champaign, IL, 2002).
- [46] L. O. Chua, *A Nonlinear Dynamics Perspective of Wolfram's New Kind of Science, vol. I-VI* (World Scientific, Singapore, 2013).
- [47] A. Ilachinski, *Cellular Automata: a Discrete Universe* (World Scientific, Singapore, 2001).
- [48] A. Adamatzky, *Identification of Cellular Automata* (Taylor and Francis, London, 1994).
- [49] H. V. McIntosh, *One Dimensional Cellular Automata* (Luniver Press, Frome, UK, 2009).
- [50] A. Wuensche and M. Lesser, *The Global Dynamics of Cellular Automata* (Addison-Wesley, Reading, MA, 1992).
- [51] T. Ceccherini-Silberstein and M. Coornaert, *Cellular Automata and Groups* (Springer Verlag, Heidelberg, 2010).
- [52] V. García-Morales, Phys. Lett. A **376**, 2645 (2012).
- [53] V. García-Morales, Phys. Lett. A **377**, 276 (2013).
- [54] E. Goles and M. Tchuente, Disc. Appl. Math. **8**, 319 (1984).
- [55] E. Goles and S. Martinez, *Neural and Automata Networks* (Kluwer, Amsterdam, 1990).
- [56] L. Yang, M. Dolnik, A. M. Zhabotinsky, and I. R. Epstein, Phys. Rev. E **62**, 6414 (2000).
- [57] S. Wolfram, Rev. Mod. Phys. **55**, 601 (1983).
- [58] V. García-Morales, Chaos Sol. Fract. **83**, 27 (2016), cond-mat/1505.02547v3.
- [59] V. García-Morales, Physica A **447**, 535 (2016), cs.OH/1507.01444v3.
- [60] V. García-Morales, arXiv:1507.08455 [nlin.CD] (2015).
- [61] V. García-Morales, A. Orlov, and K. Krischer, Phys. Rev. E **82**, 065202(R) (2010).

[62] I. Miethe, V. García-Morales, and K. Krischer, *Phys. Rev. Lett.* **102**, 194101 (2009).